ACM Technical Report ACM–TR–107

CR 151605

(NASA-CR-151605) AN ATMOSPHERIC DENSITY MODEL FOR APPLICATION IN ANALYTICAL SATELLITE THEORIES (Analytical and Computational Mathematics, Inc.) 61 p HC A04/MF A01 CSCL 22A G3/13

N78-15136

Unclas 01819

AN ATMOSPHERIC DENSITY MODEL FOR APPLICATION IN ANALYTICAL SATELLITE THEORIES

ANALYTICAL AND COMPUTATIONAL MATHEMATICS, INC.

ACM Technical Report ACM–TR–107

AN ATMOSPHERIC DENSITY MODEL FOR APPLICATION IN ANALYTICAL SATELLITE THEORIES

ANALYTICAL AND
COMPUTATIONAL
MATHEMATICS, INC.

AN ATMOSPHERIC DENSITY MODEL FOR APPLICATION IN ANALYTICAL SATELLITE THEORIES

ALAN C. MUELLER

ANALYTICAL AND COMPUATIONAL MATHEMATICS, INC.

1275 SPACE PARK DRIVE, SUITE 114,

HOUSTON, TEXAS 77058

NOVEMBER 1977

This report was prepared for the NASA/Johnson Space Center under Contract NAS9-15171.

CONTENTS

TABLES

FIGURES

AN ATMOSPHERIC DENSITY MODEL FOR APPLICATION IN ANALYTICAL SATELLITE THEORIES

by

Alan C. Mueller

1.0 INTRODUCTION

If a fully analytical satellite theory which includes the drag perturbation is to be successful, it must possess three important qualities. First, the theory should be based on a canonical formulism whereby one can use the powerful tools provided by hamiltonian mechanics. Secondly, the model used to describe the forces acting on the satellite must not be so simplified that the theory becomes only a mathematical exercise. Lastly, the resulting theory must be concise so that the accuracy gained outweighs the extra computer costs required to reach that accuracy.

Scheifele (reference 1) has developed an analytical satellite theory based on the regular, canonical Poincaré-Similar (PSϕ) elements. This is a very powerful set of elements which are in an extended phase space and have an independent variable which is similar to the true anomaly instead of time (references 2, 3 and 4). A very accurate and concise satellite theory has been developed to include the first order, short period and secular perturbations of an oblate central body. The drag theory has been built on top of the J_2 theory.

The assumption in Scheifele's theory is that the drag force is tangential to the orbit and proportional to the square of the velocity magnitude of the spacecraft. The constant of proportionality, which is a product of the density of the atmosphere, the ballistic number, and the drag coefficient, was not specified.

Since the lifting force relative to the drag force and the inertial velocity of the atmosphere relative to the satellite velocity are small, the model used by Scheifele is adequate for giving the *direction* of the retarding force due to the atmosphere. Thus an important contribution to the analytical solution was made. The report (reference 1) is a concentrated effort to canonically transform the forces into the $PS\phi$ space and also place them in a form suitable for solution. Therefore, the direction of the $PS\phi$ canonical forces has been determined but their magnitude was not completely specified. Also, the tools of hamiltonian mechanics were employed to appropriately transform the forces and reduce the size of the equations.

Numerical studies were conducted to confirm the accuracy of the resulting satellite theory. In the tests, both analytical and numerical orbit predictors assumed that the density, ballistic number (weight over projected area) and drag coefficient were constants. Results showed that the analytical and numerical solutions matched extremely well, verifying that the transformation and quadrature solution were computed properly. Due to the unique character of the $PS\phi$ system, the equations which describe the motion are relatively simple and thus satisfy the first and third above mentioned qualities.

However, for most satellites there can be extremely large changes in the density of the atmosphere along the orbit. Even for small eccentricities $(e = 0.02)$ the density can vary by a factor of 100 .

A study has been made (see section 2.0) to determine the errors that result from assuming an average constant density as compared to a density model such as that developed by Jacchia (reference 5). The comparisons point to the fact that the constant density model is adequate only for orbits of very small eccentricities. But in all the cases the analytical orbit prediction using a constant density model was much closer to the numerical prediction which used a constant density than the numerical prediction obtained by employing the Jacchia model. This implies that it is the *density model*, not the *analytical solution method*, which restricts the accuracy of the analytical theory.

Therefore the intent of this report is to develop an adequate density model and discuss the implications the model will have on the analytical drag theory. As in Scheifele's theory the ballistic number and coefficient of drag will be assumed constant.

2.0 INVESTIGATION OF CONSTANT DENSITY MODEL

If one assumes that the density of the upper atmosphere is a constant, then the drag theory and its corresponding computer program described in reference 1 are essentially complete and could be made available to the user. The question is whether or not this assumption results in solutions with acceptable errors. To answer this question a series of numerical experiments have been carried out.

Since the density is so strongly dependent on height, several orbits over a wide range of eccentricities and semimajor axes were chosen by which to test the assumption. Choosing orbits over a wide range of the other orbital elements is not a neccessity for testing the assumption.

Three *numerically* integrated solutions for the position of a satellite after a given time were determined for each of the orbit test cases. All solutions include the perturbation due to the oblate mass of the earth, but the solutions differ in their drag model. The reference solution uses an extremely accurate but complex drag model by determining the density above the oblate earth with the model developed by Jacchia. A second numerical solution was found by assuming that the density is a constant. The constant density chosen was determined by using the Jacchia model to compute the density at the coordinates of the semi-latus rectum point of the initial orbit. Lastly, a solution was obtained by completely neglecting the drag force. The "NO DRAG" and "CONSTANT" density solutions were then compared to the reference Jacchia solution and the results displayed in table I for each of the test cases. Since drag so strongly perturbs the in-track position, the differences in the solutions are given by out-of-track and in-track position errors. Also note that the out-of-track error is shown in meters while in-track error is given in kilometers.

By comparing the position differences resulting from the constant density model to the differences obtained by neglecting drag, one has a relative measure of the constant density model assumption. For instance, in all the test cases with small eccentricities the CONSTANT solution always results in smaller errors than the NO DRAG solution. This is because the height of the satellite does not vary a great deal in the orbit and thus the vehicle does not observe a large change in the density. However, the cases in which the eccentricity is somewhat larger, the satellite sees very large variations in the density and the CONSTANT solution is no better than neglecting drag completely.

The conclusion is that the constant density model results in a reasonable solution only for very small eccentricities. Even under these tight restrictions, the solutions are only labeled "reasonable", not accurate. Other factors such as the diurnal variation of the density cause the constant density assumption to be crude even for circular orbits. For these reasons, this report will concern itself with the goal of developing an accurate density model which may be inserted in the analytical theory.

TABLE I.- EVALUATION OF CONSTANT DENSITY MODEL

a (km)	e	h_p (km)	Position Differences Out of Track(m) / In Track(km) NO DRAG	CONST
6578	0.0	200	4891./172.8	710./12.0
6678	0.0	300	411./ 16.32	11./ 0.8
	0.001	293	417./ 16.48	36./ 1.6
	0.01	233	757./ 27.28	368./12.24
	0.02	166	3815./129.28	1664./46.08
6978	0.0	500	29./ 2.81	4./ 0.14
	0.001	493	29./ 2.84	3./ 0.26
	0.01	431	43./ 3.88	10./ 1.35
	0.02	363	92./ 7.68	54./ 4.72

3.0 DENSITY MODELS

In developing a density model for the analytical theory, one is severely restricted by the fact that the model must be in the form of a fourier series in the true longitude. As is the case in most analytical theories, the perturbation must be written in a fourier series to facilitate the solution of the differential equations of motion. Usually, the solution is obtained by quadrature.

Several density models have been developed to predict accurately the density at any point in space and time. Examples are the Jacchia model (reference 5) and the USSR model (reference 6). But both models are extremely complicated and too unwieldly for analytical satellite theories. In the analytical theory of Brouwer and Hori (reference 7), the density was assumed to be an exponential function of the position radius of the satellite. The exponential must then be expanded in a Poisson series so the quadrature can be performed. This model has several difficulties. It first has a problem with convergence, which Brouwer points out. Secondly, it is simply a poor model for describing the dynamic atmosphere. The density is extremely effected by such factors as the level of solar activity and whether it is summer or winter, day or night. Thus the model in Brouwer, Hori theory is simply inadequate.

Recently an extremely simple density model (referred to here as B-M) has been developed to match the Jacchia model to a high degree of accuracy (reference 8). The variations in the density due to changes in the height and changes in the relationship of the vehicle and sun position (diurnal effect) are included explicitly. Long period variations such as the changes in the average solar activity and semi-annual variations are included implicitly in the coefficients of the model. The value of the coefficients are determined by a procedure called "calibration". The simple formulation allows the model to be inverted, i.e. given the density at different points in space (as determined from Jacchia) one can compute the coefficients of the B-M model. Since the coefficients are implicit functions of long period effects, they can be considered constants over a limited period of about a month.

Even this extremely simple model cannot be applied in the analytical drag theory because it cannot be written in the form of a fourier series. However the technique of the B-M model does give important insight and direction to follow.

In all the models discussed, the representations of the density are considered to be global. In other words, given any position in the atmosphere one can determine its density. The approach, to be taken here, is to develop a model which expresses the density along a particular orbit. The coefficients in the model will be calibrated with the Jacchia model in a manner similar to the B-M model. But in this case, the coefficients in the model are not only implicit functions of the long period variations in the atmosphere but also the orbital elements which describe the orbit. The result is a density model which can be written in a fourier series and easily implemented into the drag theory. Since the orbital elements are perturbed by J_2 and drag, the coefficients in the model must be updated periodically or corrected in some manner to reflect the changes. Since the perturbations are small, the updating would be infrequent.

3.1 Development of the Model

In the B-M model, the variations in the density due to the height and diurnal effect are modeled as

$$\rho = \exp\left(T(h) + \underbrace{S(h) * g^m(\alpha_s, \delta_s, \alpha_v, \delta_v)}_{\text{diurnal term}}\right) \qquad (1)$$

where

ρ = density

$T(h)$ = function of altitude (nighttime vertical profile)

$S(h)$ = function of altitude (diurnal magnitude)

$g(\alpha_s, \delta_s, \alpha_v, \delta_v)$ = function of right ascension and declination of the sun and vehicle.

And similarly the USSR model is expressed as

$$\rho = \exp\left(T'(h)\right) * \left(1 + S'(h) * g^m (\alpha_s, \delta_s, \alpha_v, \delta_v)\right) \qquad (2)$$

where

$T'(h)$ = function of altitude (nighttime vertical profile)

$S'(h)$ = function of altitude (diurnal magnitude).

Both models point to the fact that the density may be expressed in such a form as

$$\rho = T^*(h) + S^*(h) \cdot g^m (\alpha_s, \delta_s, \alpha_v, \delta_v) \qquad (3)$$

where T^* and S^* are functions of the height and g is a simple function of the angular coordinates of the sun and vehicle. If the oblate figure of the earth is neglected, then T^* and S^* may be assumed to be functions of the vehicle position radius.

In the PSϕ† element system the radius is described as follows

$$r = \frac{p}{1+e \cos \phi} = \frac{p}{1+\sqrt{1-\frac{\eta^2}{2}}\ \zeta_1} \qquad (4)$$

where p is approximately the semi-latus rectum and η is proportional to the eccentricity, and ζ_1 is given by

---

† The PSϕ action variables are ρ_1, ρ_2, ρ_3, ρ_4 and their canonical conjugate variables are σ_1, σ_2, σ_3, σ_4.

$$\zeta_1 = \beta(\rho_2 \, cos \; \sigma_1 - \sigma_2 \, sin \; \sigma_1) \quad , \quad \beta^2 = \frac{\sqrt{2\zeta_4}}{\mu}$$

The radius can be expanded about p if the eccentricity is considered small, i.e.

$$r = p \sum_{i=o}^{n} e_i(\eta) \, \zeta_1^i \tag{5}$$

where e_i are functions of η

Since T* and S* are functions of the radius, this suggests they too may be described in a similar manner

$$T^*(h) = \sum_{i=o}^{n} a_i' \, \zeta_1^i \tag{6}$$

$$S^*(h) = \sum_{i=o}^{n} b_i' \, \zeta_1^i \tag{7}$$

where the coefficients a_i' and b_i' are implicit functions of the eccentricity, semi-latus rectum p , and the character of the atmosphere.

Neglecting small terms in the angular function $g(\alpha_s, \delta_s, \alpha_v, \delta_v)$ the USSR model gives

$$g^m = \left(\frac{1 + cos \; \psi}{2} \right)^{\frac{m}{2}} \tag{8}$$

where

$$cos\psi = \frac{1}{r} \left(z \cdot sin \; \delta_s + cos \; \delta_s \cdot (x \cdot cos \; \gamma + y \cdot sin \; \gamma) \right)$$

$$\gamma = \alpha_s + \phi$$

x, y, z = defines position of satellite

(α_s, δ_s) = right ascension and declination of sun

ϕ = defines lag of the density bulge behind the sun ($\phi \simeq 37°$).

The power of exponent m ranges near the value of 4. If $m = 4$ is chosen then $g^m(\alpha)$ can be expressed as a fourier series in the PSϕ elements

$$d' = g^4(\alpha) = d_0 + d_1 \, sin \, \sigma_1 + d_2 \, cos \, \sigma_1 + d_3 \, sin \, 2\sigma_1 + d_4 \, cos \, 2\sigma_1 \tag{9}$$

where

$$d_0 = \frac{2+D^2+E^2}{8} \qquad d_3 = D \cdot \frac{E}{4}$$

$$d_1 = \frac{E}{2} \qquad d_4 = \frac{(D^2-E^2)}{8}$$

$$d_2 = \frac{D}{2}$$

$$\begin{aligned} D &= \sigma_3 B + cos \, \delta_s \, cos \, \gamma \\ E &= - \zeta_3 B + cos \, \delta_s \, sin \, \gamma \\ B &= \frac{1}{2G} \left[sin \, \delta_s \sqrt{2(G+H)} - cos \, \delta_s (\sigma_3 \, cos \, \gamma + \rho_3 \, sin \, \gamma) \right] \end{aligned} \tag{10}$$

The coefficients d_i can be considered constants over a few revolutions. But due to the fact that the position of the sun changes and the orbital elements are perturbed, an infrequent update will be required to reflect these changes.

Thus the total model for the density along the initial orbit follows from equations (3), (6), (7) and (9)

$$\rho_0 = \sum_{i=o}^{n} (a_i + d \, b_i) \, \zeta_1^i \tag{11}$$

where

$$a_i = a_i' + d_o b_i' \qquad\qquad b_i = b_i' \tag{12}$$
$$d = d' - d_o$$

The coefficients a_i and b_i can be determined by a calibration with Jacchia. A linear system of $2(n+1)$ equations with $2(n+1)$ unknowns must be solved to determine the coefficients.

3.2 Density Model Corrections

The density model proposed in section 3.1 reflects the observed density variations due to the two-body changes in the height and due to the varying angle between the sun and the satellite. Santora (reference 9) also considers two additional phenomena that effect the height of the satellite which in turn causes variations in the observed density. One effect is the changes in the height due to oblate figure of the earth. For instance, a satellite in a circular orbit about the equator will see no changes in the height, but a satellite in a circular, polar orbit will find that its height will change by about 20 km. These changes in height translate to a substantial variation in the observed density of about 50% Secondly, changes in the height due to the J_2 periodic oscillations in the radius can also result in large variations in the observed density.

Both of these effects may be modeled as corrections to the model proposed in section 3.1:

$$\rho = \rho_o \; e^{\alpha \Delta h} \tag{13}$$

where Δh is the change in the height due to the above mentioned effects, ρ_o is given by equation (11) and ρ is the corrected density. The constant α is an implicit function of the character of the atmosphere and may be determined easily by calibration with the Jacchia model. For small changes in height, one can expand and truncate equation (13) which results in

$$\rho = c\rho_0 \quad , \quad c = 1 + \alpha\Delta h \tag{14}$$

The oblate figure of the earth can be described by

$$R = R_e \left(1+\delta\left(\frac{Z}{r}\right)^2\right)^{-\frac{1}{2}} \tag{15}$$

where R is the radius at an arbitrary point on the earth

R_e is the mean radius at the equator

δ is the bulge parameter

$(\frac{Z}{r})$ determine the latitude of the point.

Since δ is small ($\delta \simeq 0.67\text{x}10^{-2}$) equation (15) can be expanded and truncated to give

$$R = R_e \left(1-\tfrac{1}{2}\delta\left(\frac{Z}{r}\right)^2\right) \tag{16}$$

The latitude term may be expressed in the $PS\phi$ element as

$$\left(\frac{Z}{r}\right)^2 = \frac{G+H}{4G^2}\left(\sigma_3^2 + \rho_3^2 + 2\sigma_3\rho_3 \, \mathit{sin}\ 2\sigma_1 + (\sigma_3^2-\rho_3^2)\ \mathit{cos}\ 2\sigma_1\right) \tag{17}$$

Thus if one defines the mean radius as observed by a satellite in its orbit as R_m

$$R_m = R_e \left[1 - \delta \frac{(G+H)}{8G^2} (\sigma_3^2+\rho_3^2)\right] \tag{18}$$

Then the oscillation of the height about the mean radius is given by

$$\Delta h_R = R_e \frac{\delta(G+H)}{8G^2}\left[2\sigma_3\rho_3 \, sin \, 2\sigma_1 + (\sigma_3^2-\rho_3^2) \, cos \, 2\sigma_1\right] \qquad (19)$$

Derivation of the change in height due to the J_2 term is somewhat more lengthy but can be simplified by neglecting terms on the order of the eccentricity. Since the oscillations in the height due to J_2 have a magnitude of about 5 km and because the drag theory is restricted to $e \simeq 0.1$, neglecting order O(e) terms results in errors of at most 500 meters. This results in a negligible error in the density computation.

The change in height due to J_2 can be found by differencing the radius computed from the mean elements r' from the actual radius r :

$$\Delta r = r - r' \qquad (20)$$

where

$$r' = \frac{p'}{1+Q'Z_1'} \qquad r = \frac{p}{1+QZ_1}$$

Primed variables are based on the primed (mean) PSϕ elements (see reference 4). Neglecting O(e) terms, the difference becomes

$$\Delta r = p(1-QZ_1) - p'(1-Q'Z_1') \qquad (21)$$

If one defines relations between primed and unprimed values as

$$\begin{aligned} p &= p' + \Delta p \\ Q &= Q' + \Delta Q \\ Z_1 &= Z_1' + \Delta Z_1 \end{aligned} \qquad (22)$$

then Δp, ΔQ and ΔZ_1 can be found from relations derived from the generating function S_1 used in eliminating short periodic effects (reference 4).

From the relation for the semi-latus rectum p in terms of PSϕ elements,

$$p = \frac{1}{\mu} \left[-\tfrac{1}{2}(\sigma_2^2+\rho_2^2) + \frac{\mu}{\sqrt{2\rho_4}} \right]^2 \tag{23}$$

one can linearly approximate Δp as

$$\Delta p = -\sqrt{\frac{p}{\mu}} \left[\sigma_2 \Delta\sigma_2 + \rho_2 \Delta\rho_2 + \frac{\mu}{(2\rho_4)^{\frac{3}{2}}} \Delta\rho_4 \right] \tag{24}$$

The deviations $\Delta\sigma_2$, $\Delta\rho_2$ and $\Delta\rho_4$ can be found directly from the partials of S_1 . But Δp is of the order $0(e)$ since σ_2 and ρ_2 are eccentricity terms and $\Delta\rho_4 = 0$ because of the use of total energy elements. A similar argument can be made for ΔQ . And thus Δr reduces to

$$\Delta r = pQ\Delta Z_1 + 0(e) \tag{25}$$

From the expression for Z_1

$$Z_1 = \rho_2 \cos \sigma_1 - \sigma_2 \sin \sigma_1 \tag{26}$$

one can approximate ΔZ_1 as

$$\begin{aligned} \Delta Z_1 = {} & \Delta\rho_2 \cos \sigma_1 - \Delta\sigma_2 \sin \sigma_1 \\ & - \Delta\sigma_1 (\rho_2 \sin \sigma_1 + \sigma_2 \cos \sigma_1) \end{aligned} \tag{27}$$

Neglecting terms of $O(e)$

$$\Delta Z_1 = \Delta\rho_2 \cos \sigma_1 - \Delta\sigma_2 \sin \sigma_1 \tag{28}$$

By a rather lengthy but straight forward derivation one finds, through use of the generating function S_1 , that $\Delta\dot{Z}_1$ can be expressed as

$$\Delta Z_1 = \varepsilon \frac{w}{3G^2}\left(G^2 - 3H^2 + s \sin 2\sigma_1 + c \cos 2\sigma_1\right) \tag{29}$$

where ε is the J_2 perturbing parameter defined in reference 4 and

$$\begin{aligned} w &= \frac{Q}{2pq} \\ s &= -(G+H)\,\sigma_3\rho_3 \\ c &= (G+H)\,\frac{(\rho_3^2-\sigma_3^2)}{2} \end{aligned} \tag{30}$$

If one defines the average radius r_a as

$$r_a = r' + \frac{\varepsilon pQw}{3G^2}(G^2-3H^2) \tag{31}$$

then the oscillation in the height due to J_2 is given by

$$\Delta h_{J_2} = \frac{-\varepsilon pQw}{6G^2}(G+H)\left(2\sigma_3\rho_3 \sin 2\sigma_1 + (\sigma_3^2-\rho_3^2) \cos 2\sigma_1\right) . \tag{32}$$

It is interesting to note the similarities in the equation for the change in height due to the dynamics (eq.(32)) and the geometry (eq.(19)). Both the oscillations will have two peaks and two valleys, except their magnitudes are different and are 90^0 out of phase. Also, both oscillations vanish when the inclination goes to zero. Thus the model given by equation (14) can be expressed as

$$\rho = \rho_o \left[1 + \kappa \left(2\sigma_3\rho_3 \, \mathit{sin} \, 2\sigma_1 + (\sigma_3^2 - \rho_3^2) \, \mathit{cos} \, 2\sigma_1\right)\right] \tag{33}$$

where

$$\kappa = \alpha \frac{(G+H)}{2G^2} \left[\frac{R_e \delta}{4} - \frac{\varepsilon p Q w}{3} \right] \tag{34}$$

The coefficients in ρ_0 (equation (11)) are computed with the primed PSϕ elements by a calibration to the Jacchia model, as described in Section 3.1. The height used to evaluate the Jacchia model is given by the difference between the average radius r_a and the mean radius of the earth seen by the satellite

$$h = r_a - R_m$$

$$h = r' + \frac{\varepsilon p Q w}{3G^2} (G^2 - 3H^2) - R_e \left[1 - \frac{\delta (G+H)}{8G^2} (\sigma_3^2 + \rho_3^2)\right] \tag{35}$$

3.3 Model Verification

To verify that the proposed density model has an adequate accuracy, a set of experiments have been conducted to compare the new model with the Jacchia model.

In all of the tests, the density as observed along different points of a J_2 perturbed orbit about the oblate earth is computed with the Jacchia model and then compared with the new model. A value of 4 was chosen for n (eq.(11)) so that ρ_0 has 10 coefficients to be determined by calibration. A matrix inversion algorithm (reference 10) was used to solve for the value of the coefficients.

Several different orbits and sun conditions were chosen by which to compare the new models. These cases have all been labeled in Table II and will be referred to in the discussion of the comparisons.

The first comparison of the two models is intended to demonstrate that extremely large variations in the density due to the solar activity level, $F_{10.7}$, can be accounted for by the new model's technique of calibration.

In figure 1(a), the density is plotted versus the true longitude of the satellite. Two graphs are shown, one as determined from Jacchia, and the other as found from the new model. The initial conditions are given by Case 1 in Table II. The resulting differences between the two models are never greater than three percent. In figure 1(b), another two graphs are shown except with initial conditions given by Case 2. Again the models are in good agreement. The only difference between case 1 and 2 is their solar flux values; but notice the large quantitative differences between the density plots in figures 1(a) and 1(b). The new model is able to account for these very important differences.

The second comparison demonstrates the ability of the new model to account for density variations due to the changing position of the sun. Again in figure 2, the density is plotted versus the true longitude. There are four plots on figure 2 representing the two different models and two different initial conditions given by case 3 and 4. The only difference between these cases is the position of the sun. In case 3 the sun is in the first day of summer while in case 4 the sun is in the first day of spring (vernal equinox). Here too one finds that the new model is able to reflect the differences.

The four remaining comparisons are intended to show that the proposed model simulates the Jacchia model for a variety of orbits and to demonstrate the errors resulting from neglecting the effects of the diurnal bulge, the oblate figure of the

TABLE II.- TEST CASES

	Case 1	Case 2	Case 3	Case 4	Case 5	Case 6	Case 7
a(km)	6978	6978	6678	6678	6978	6678	6978
h_p(km)	600	600	300	300	600	233	460
e	0.0	0.0	0.0	0.0	0.0	0.01	0.02
I	90^0	90^0	90^0	90^0	90^0	90^0	90^0
ω	0^0	0^0	0^0	0^0	0^0	0^0	0^0
Ω	90^0	90^0	90^0	90^0	90^0	90^0	90^0
M	20^0	20^0	20^0	20^0	20^0	20^0	20^0
Sun	Summer	Summer	Summer	Spring	Summer	Summer	Summer
$\overline{F}_{10.7}$	75	250	180	180	180	180	180

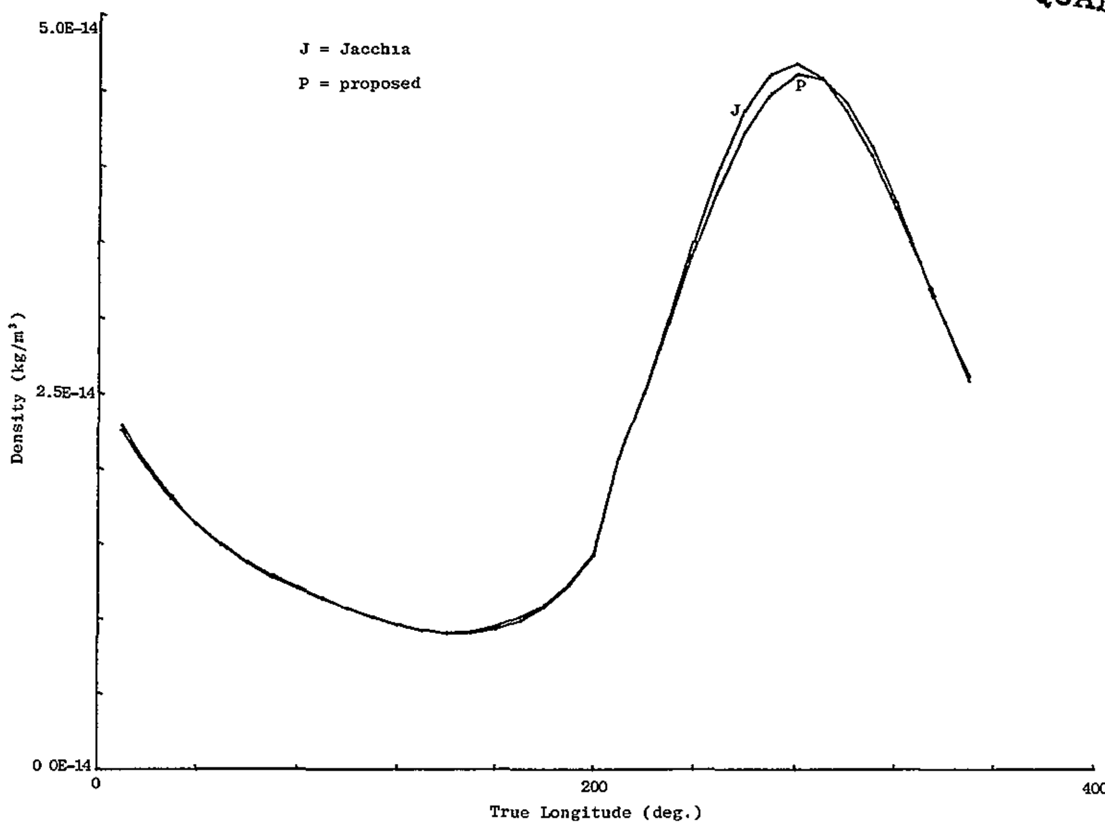

FIGURE 1(a) Density Variations, Case 1

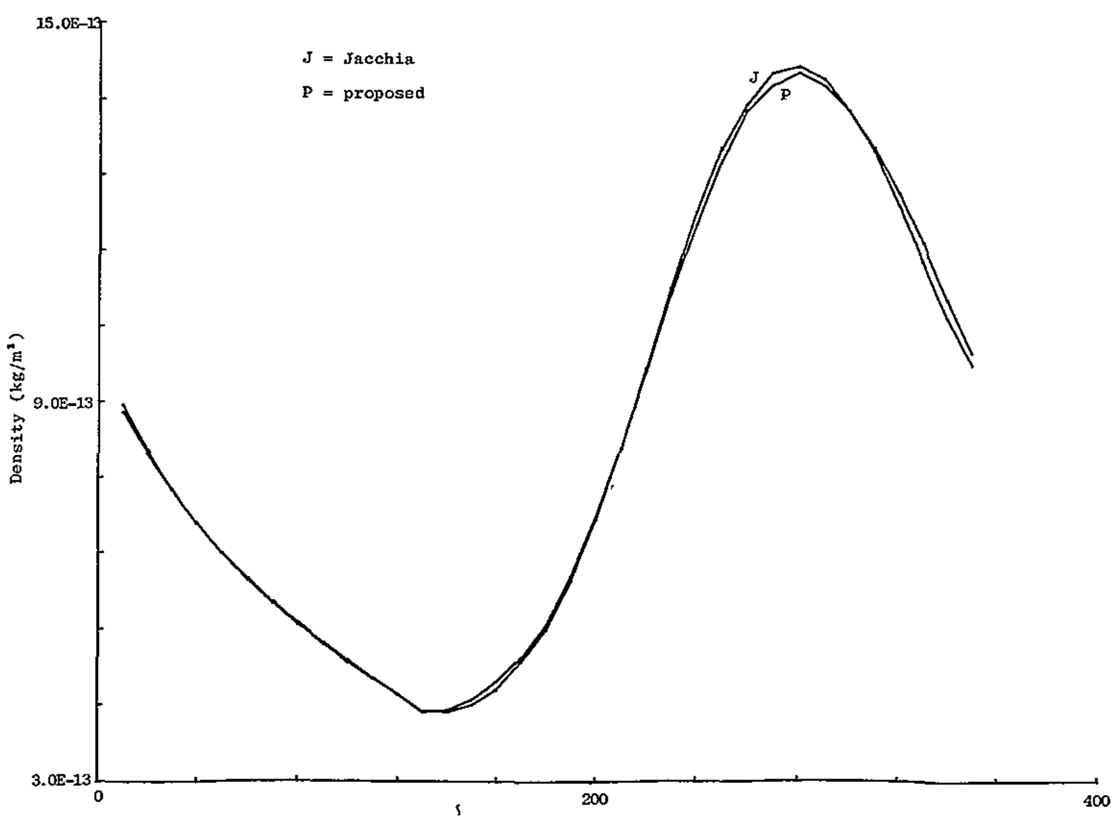

FIGURE 1(b): Density Variations, Case 2

ORIGINAL PAGE IS
OF POOR QUALITY

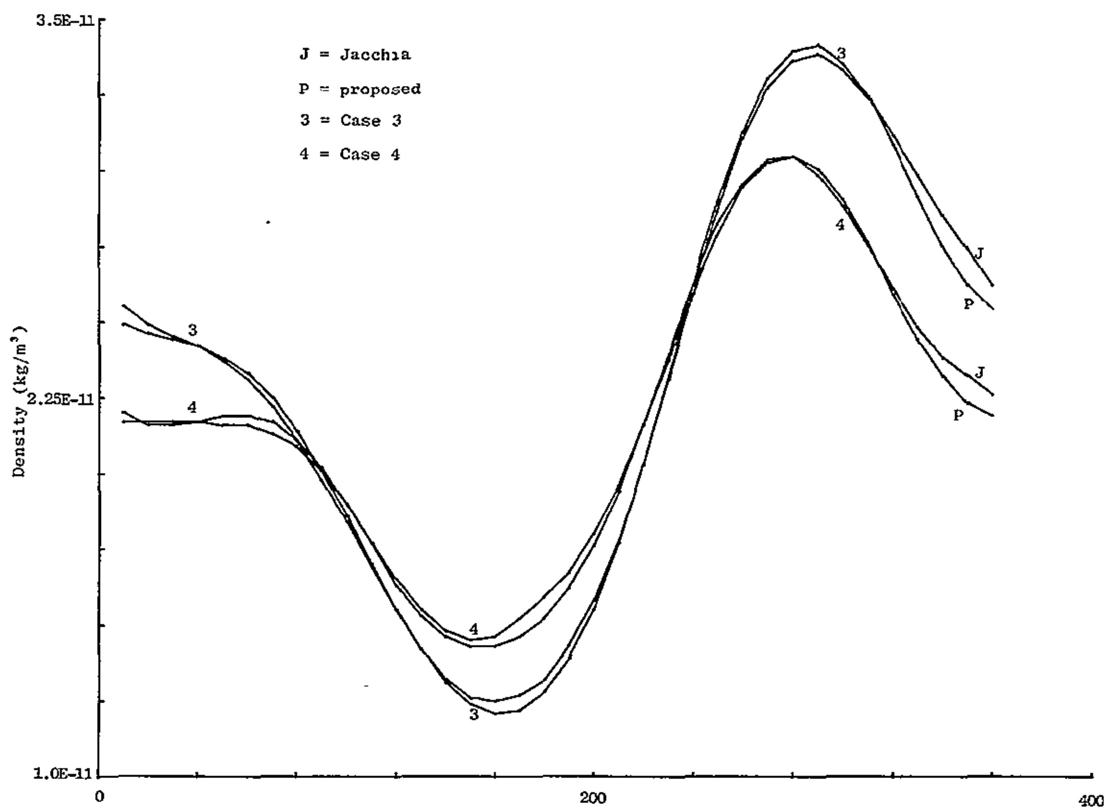

FIGURE 2· Density Variations, Case 3 and 4

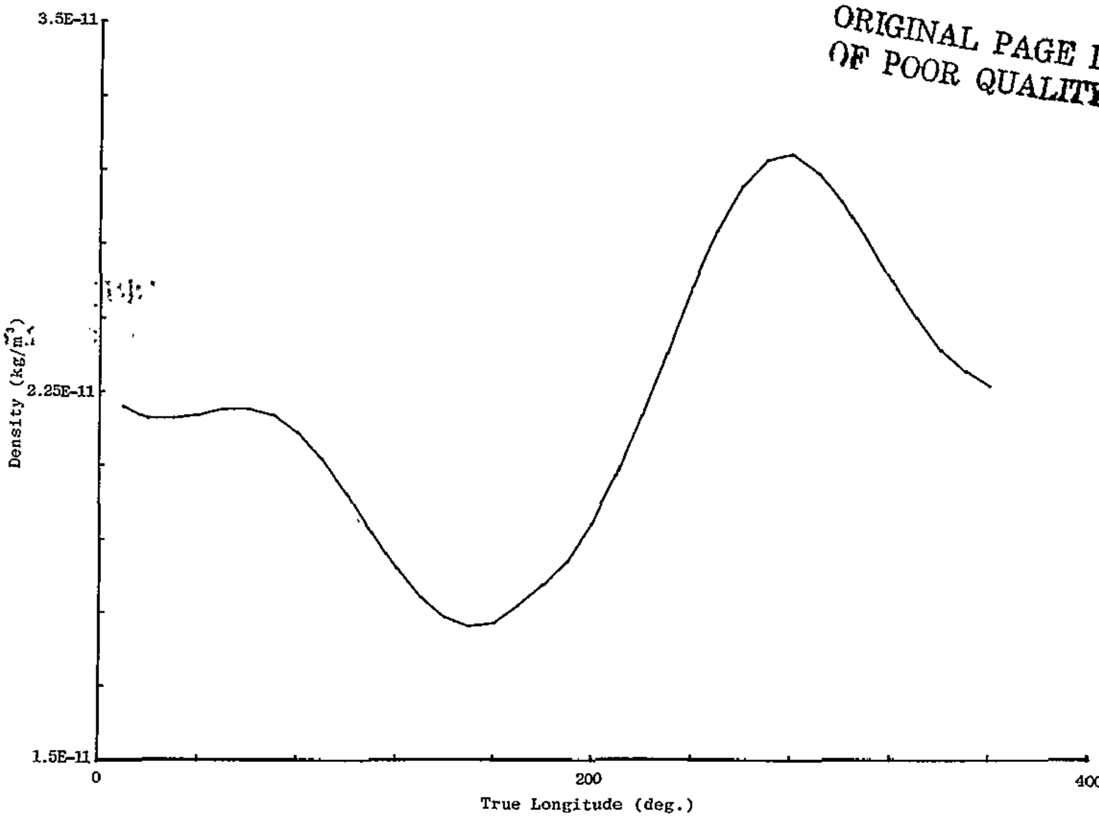

FIGURE 3(a): Density Variations, Case 4

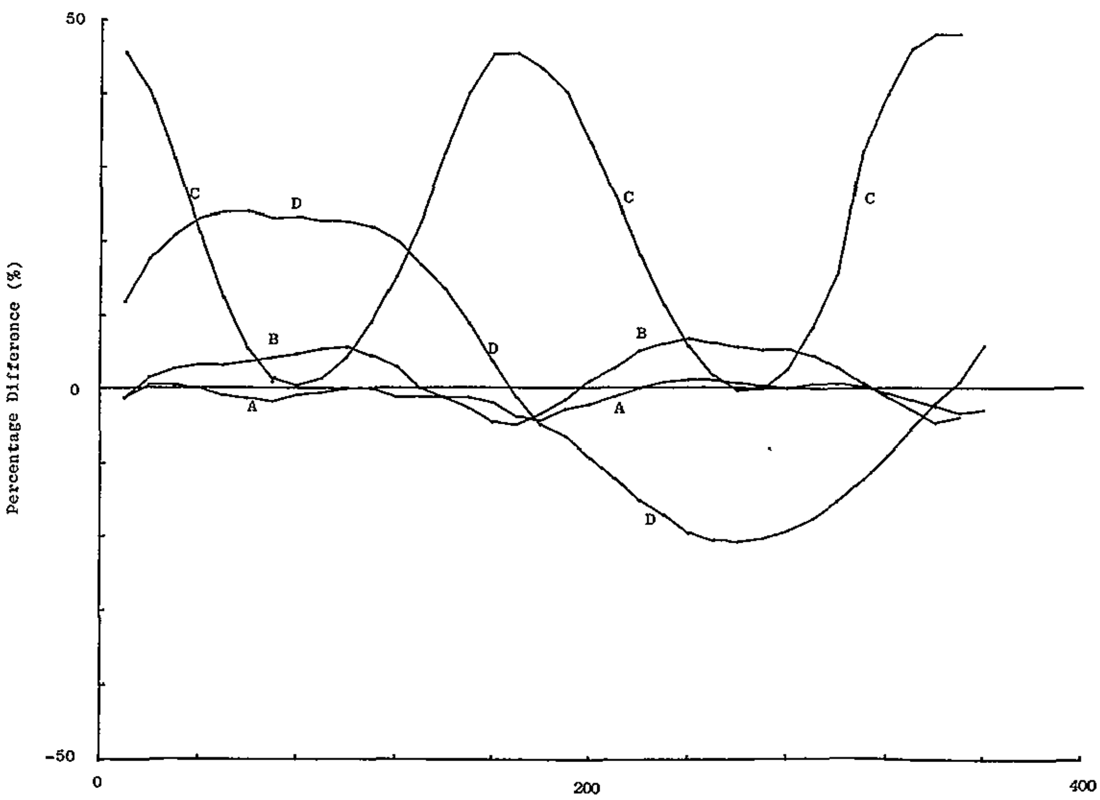

FIGURE 3(b): Percentage Difference in the Models, Case 4

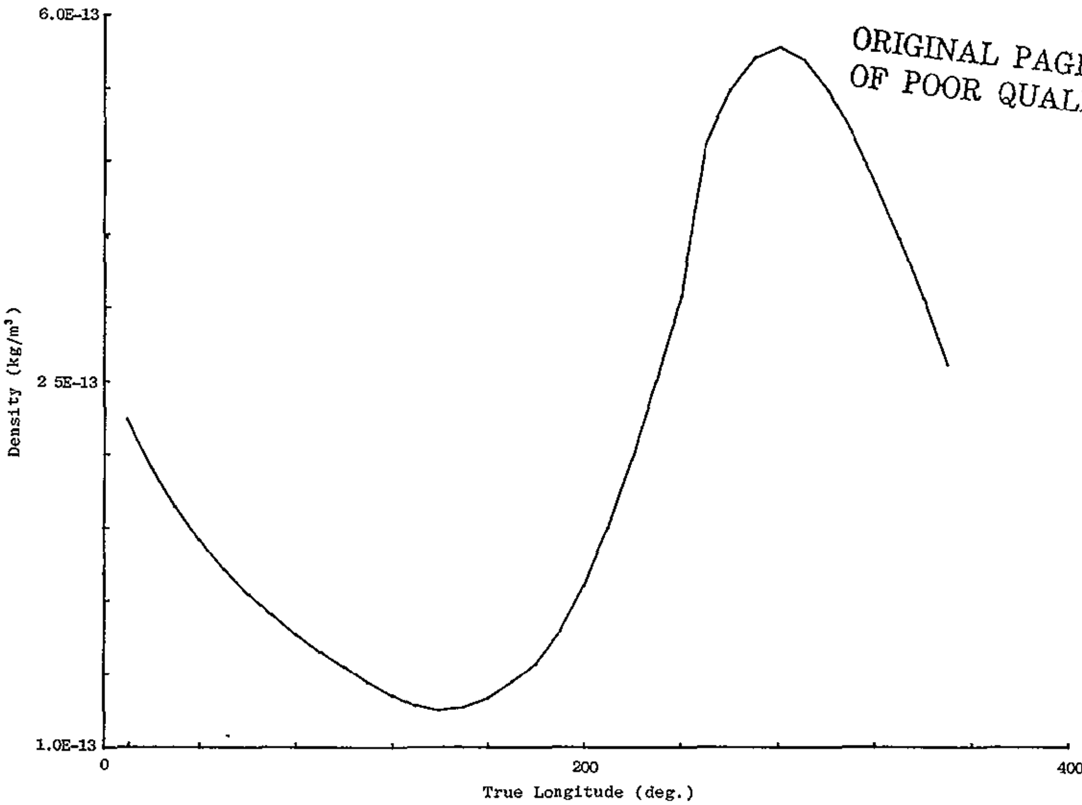

FIGURE 4(a): Density Variations, Case 5

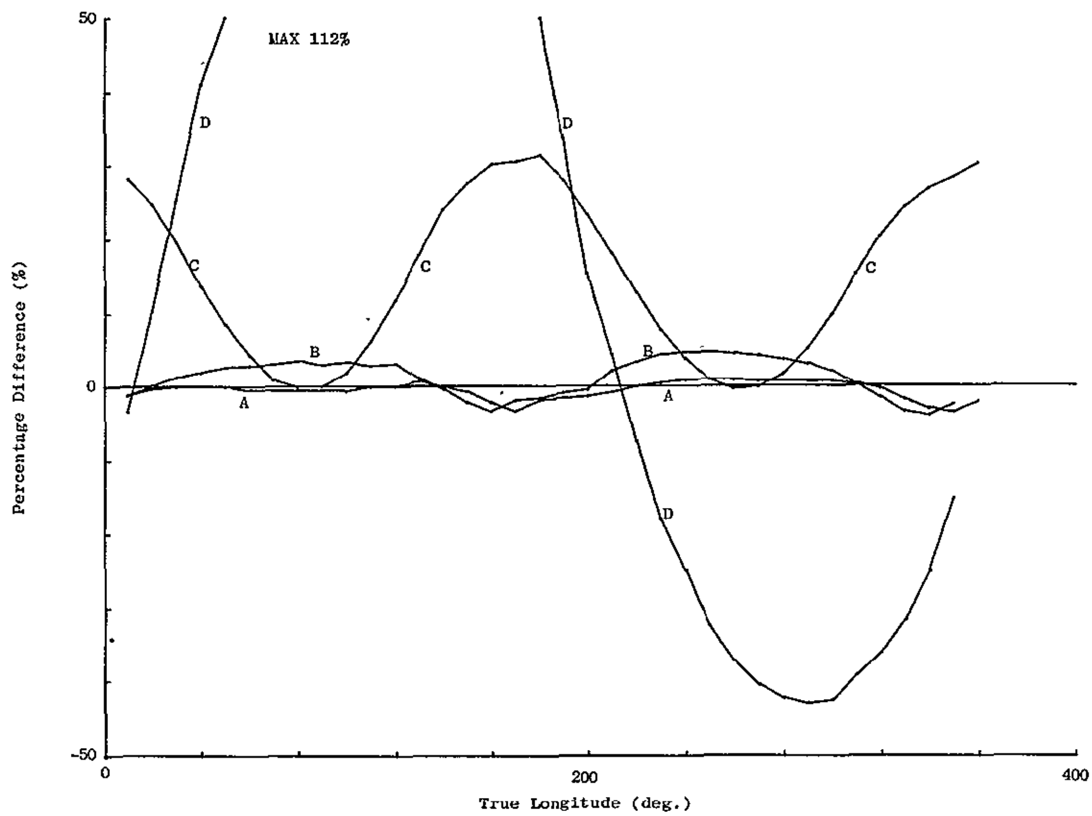

FIGURE 4(b): Percentage Difference in the Models, Case 5

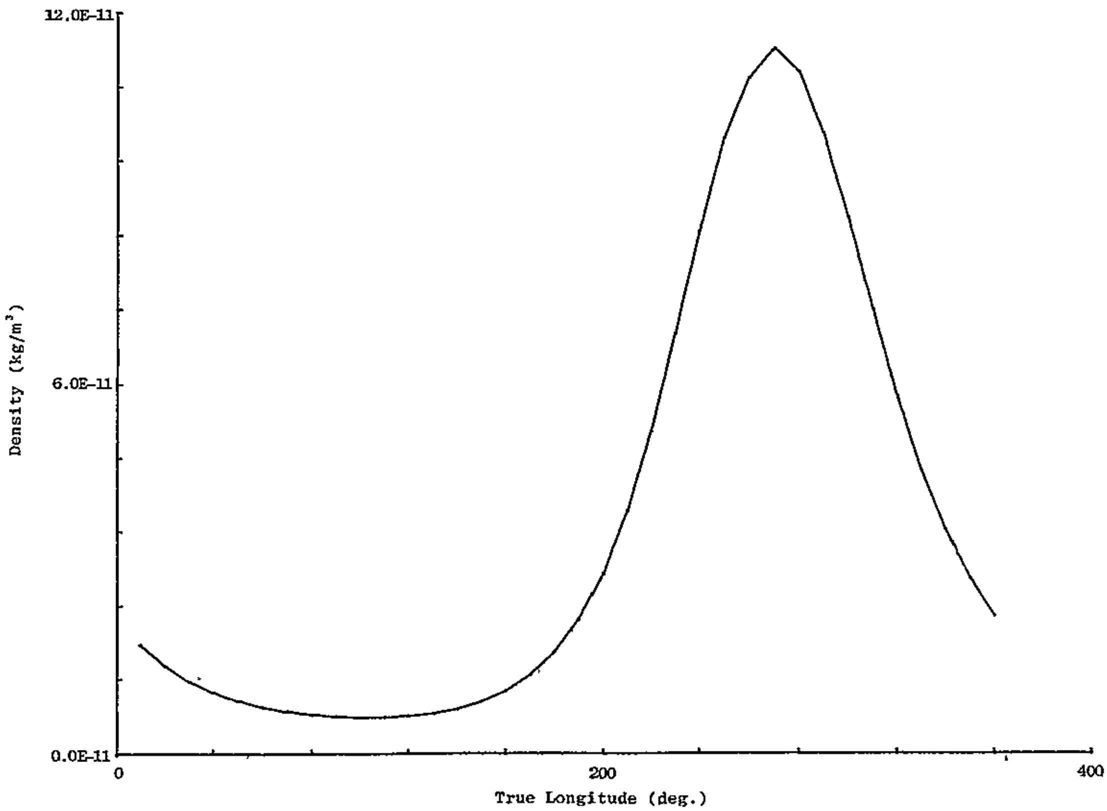

FIGURE 5(a): Density Variations, Case 6

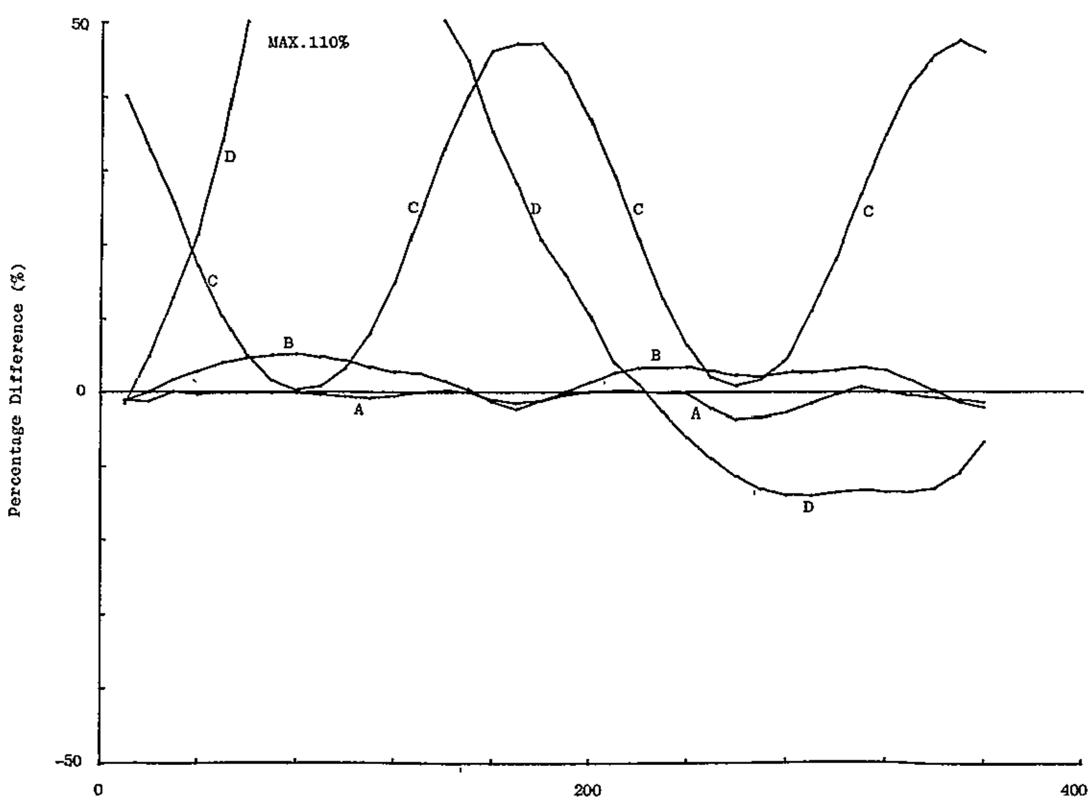

FIGURE 5(b). Percentage Difference in the Models, Case 6

ORIGINAL PAGE IS
OF POOR QUALITY

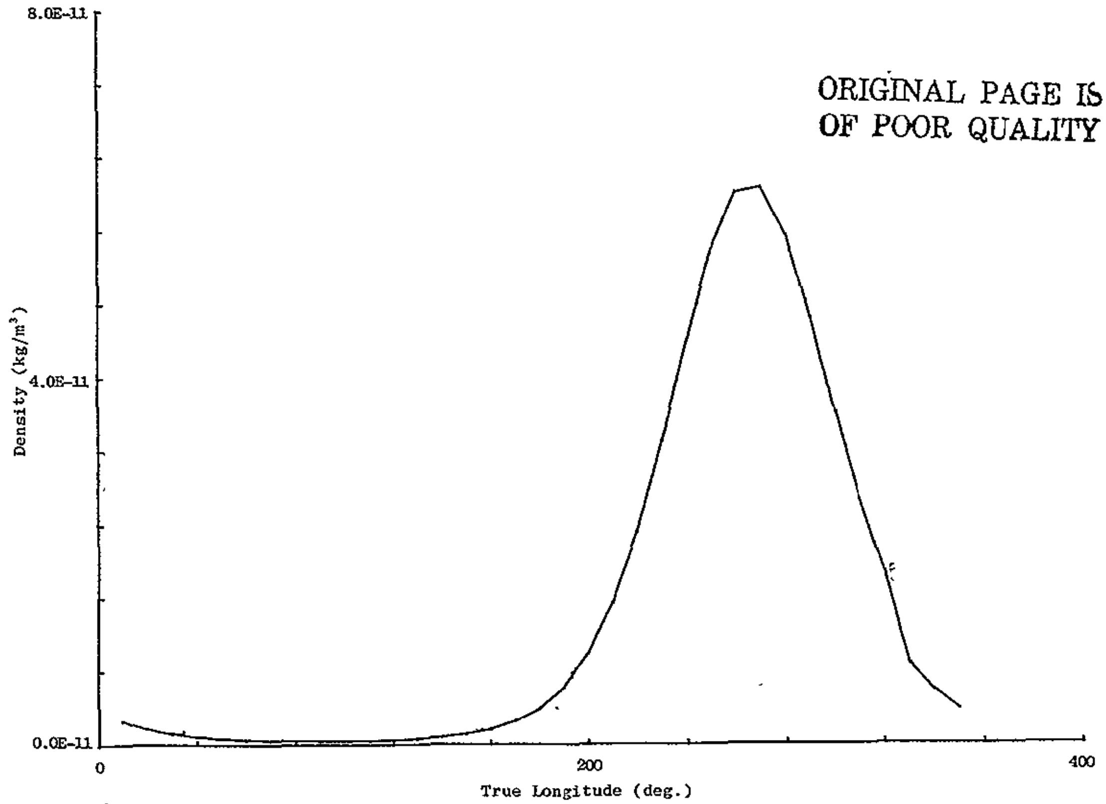

FIGURE 6(a). Density Variations, Case 7

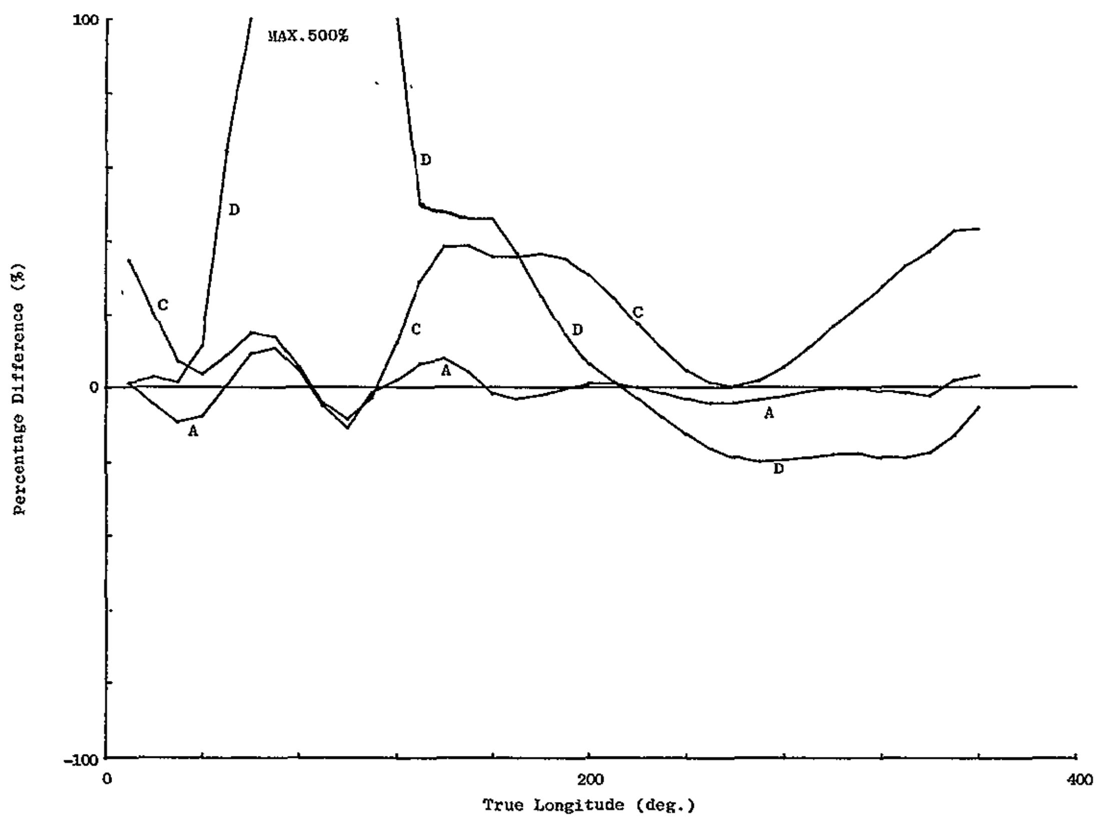

FIGURE 6(b). Percentage Difference in the Models, Case 7 earth, or the J_2 periodic oscillations in the radius. In figures 3(a),4(a),5(a) and 6(a), the density as determined from Jacchia is plotted versus the true longitude, corresponding to the test cases 4 through 7. These peculiar and varied graphs give a clear picture of the problem of developing the density (vertical axis) as a fourier expansion of the true longitude (horizontal axis). Be careful to note the changes in the scale for the density axis for the four different plots.

In figures 3(b),4(b),5(b) and 6(b), the percentage difference between the new model and Jacchia is plotted versus the true longitude. In each figure there are four plots labeled A, B, C and D. The D plot is the differences resulting from the new model if the diurnal effect is neglected. Similarly the C plot is from neglecting the oblate figure of the earth and the B plot is from neglecting the J_2 radius oscillations. Finally the A plot is the resulting differences if the complete model is used.

Case 4 is a circular, polar orbit and thus the density variations seen in figure 3(a) are due entirely to the diurnal effect and the changes in the height because of the oblate figure and mass of the earth. The rather strange appearance of the plot is a result of the cancellation and addition of the different effects. From figure 3(b) one finds large errors result if diurnal or oblate figure effects are neglected. Smaller errors result from neglecting the J_2 oscillations. As expected, the oblate mass and oblate figure effects have two peaks and valleys and are 90^0 out of phase. Also note that the errors in plot C are always positive. The reason for this behavior is because the earth's radius was assumed to be a constant equatorial radius which is larger than at the poles. The result is that a greater density is predicted for every point except when the satellite crosses the equator. The residual errors from the total model are always less than three percent.

Case 5 is also a circular, polar orbit but has an altitude of about 300 km. greater than in case 4. The density plot of this case is shown in figure 4(a) and the differences are plotted in figure 4(b).

The neglecting of the diurnal effect results in the largest errors. The differences between the magnitude of the errors in plot C in figures 3(b) and 4(b) reflect the fact that the diurnal effect becomes more prominent for higher altitudes. The other plots show the same pattern as in case 4 and again the total model exhibits small errors.

Case 6 is a polar orbit with what appears to be a relatively small eccentricity. Actually this small eccentricity translates to a very large density variation. In figure 5(a) the major variation in the density is due to the variation in height of the elliptical orbit. But by examination of the error plots in figure 5(b), one finds the other effects are also very important - especially the diurnal effect.

Case 7 is also a polar orbit with an eccentricity which results in density variations of 4.22×10^{-13} to $6.03 \times 10^{-11} \frac{kg}{m^3}$, a factor of over 100. Here the plot in figure 6(a) begins to look more like an impulse where the satellite experiences large densities only near its perigee point. The scale of the vertical axis in figure 6(b) has been changed to show the very large errors resulting from neglecting the diurnal effect. Plot B has not been shown because the scale does not bring out the differences between plots A and B .

Errors in plot A become as large as ten per cent but this is only when the satellite sees its smallest densities at the apogee.

As the eccentricity of the orbit increases, the plot of the density versus true longitude begins to look more and more like an impulse. The result is that for eccentricities of $e > 0.03$ the model begins to break down. The fourier series cannot converge when modeling the impulse.

However, this is not such a severe restriction. Most near earth satellites have eccentricities well within the $e = 0.03$. For satellites with greater eccentricities one may avert this problem in a manner similar to that described by Watson (reference 12). The density can be modeled only in the region near the perigee point where it is largest. The analytical integration then proceeds in steps.

From these results, it is concluded that the proposed model is quite suitable for applications in the analytical theory. It matches the Jacchia model extremely well and is easily written in the form of a fourier series.

3.4 Second Order Corrections

Because the density is so strongly dependent on the height, it is important that changes in the height are accounted for. The proposed model accounts for the two-body and J_2 changes in height and also the changes due to the oblate figure of the earth. But the drag force itself causes a secular perturbation in the height. For very high satellites, the perturbation is small and can be neglected in the density considerations. But for satellites which pass through the dense atmosphere, the effect is much like a snowball growing as it falls down the hill. The drag force causes the satellite to dip deeper in the atmosphere where the more dense air causes a stronger drag force and so on. Once again this effect can be modeled as a correction as in equation (13)

$$\rho = (1 + \alpha\Delta h) \cdot \rho_0 \tag{36}$$

If one assumes that the drag perturbs the radius of the satellite orbit in a secular manner and neglects the terms on the order of the eccentricity, then the change in height can be related to the perturbation in the semi-latus rectum, i.e.

$$\Delta h = \Delta p \tag{37}$$

Since the p is given by

$$p = \frac{1}{\mu}\left[-\tfrac{1}{2}(\sigma_2^2+\rho_2^2) + \frac{\mu}{(2\rho_4)^{\frac{1}{2}}}\right]^2$$

then the deviations due to drag can be written as

$$\Delta p = -\left(\frac{p}{\mu}\right)^{\frac{1}{2}}\left(\sigma_2\Delta\sigma_2 + \rho_2\Delta\rho_2 + \frac{\mu}{(2\rho_4)^{3/2}}\Delta\rho_4\right) \tag{38}$$

But neglecting eccentricity terms and assuming a secular drag perturbation in the energy ρ_4 one finds

$$\Delta p = \left(\frac{\Delta p}{\Delta\tau}\right)\tau = \left(-(\mu p)^{\frac{1}{2}} \cdot \frac{1}{(2\rho_4)^{3/2}}\frac{\Delta\rho_4}{\Delta\tau}\right)\tau \tag{39}$$

where $\dfrac{\Delta\rho_4}{\Delta\tau}$ is the rate of change in the energy due to drag.

Initially $\dfrac{\Delta\rho_4}{\Delta\tau}$ may be determined by neglecting the effect of drag on the atmosphere density model. Once this guess is made, one can re-evaluate the changes in the elements based on the complete model.

3.5 Density Model Summary

From the theoretical developments in this section, the complete proposed density model may be written as

$$\rho = \left[1 + \left(\alpha \frac{\Delta p}{\Delta \tau}\right) \tau + \alpha \Delta h\right] \rho_0$$

where

$$\Delta h = \kappa\left[2\sigma_3\rho_3 \ sin\ 2\sigma_1 + (\sigma_3^2 - \rho_3^2)\ cos\ 2\sigma_1\right]$$

$$\frac{\Delta p}{\Delta \tau} = \frac{-1}{2\rho_4}\sqrt{\frac{\mu p}{2\rho_4}} \quad \frac{\Delta \rho_4}{\Delta \tau}$$

$$\kappa = \frac{G+H}{2G^2}\left(\frac{R_e \delta}{4} - \frac{\varepsilon p Q w}{3}\right)$$

$$\rho_0 = \sum_{i=1}^{n} (a_i + db_i)\ \zeta_1^i$$

$$d = d_1\ sin\ \sigma_1 + d_2\ cos\ \sigma_1 + d_3\ sin\ 2\sigma_1 + d_4\ cos\ 2\sigma_1$$

$$d_1 = \frac{E}{2} \qquad d_3 = D \cdot \frac{E}{4}$$

$$d_2 = \frac{D}{2} \qquad d_4 = \frac{(D^2 - E^2)}{4}$$

$$D = \sigma_3 B + cos\ \delta_s\ cos\ \gamma$$

$$E = -\rho_3 B + \cos \delta_s \sin \gamma$$

$$B = \frac{1}{2G} \left[\sin \delta_s \sqrt{2(G+H)} - \cos \delta_s (\sigma_3 \cos \gamma + \rho_3 \sin \gamma) \right]$$

$$\gamma = \alpha_s + \phi$$

α_s , δ_s : right ascension and declination of sun

ϕ : defines lag of diurnal bulge behind sun

δ : measure of geometric oblateness of earth

ε : perturbing J_2 parameter

a_i , b_i : model parameters found by calibration

4.0 DENSITY MODEL IMPLICATIONS ON DRAG THEORY

The proposed density model requires a number of fourier expansions in addition to those developed for the constant density case in reference 1. The addition of the new density model in the analytical theory does not, however, require any new Taylor series expansions which were processed by the computer logic described in that reference. Thus the discussion here will be concerned with the new fourier expansions that are needed.

In the discussion of the power series expansion, one must make a distinction between the expansions of the properties of the orbit (such as the radius, time and velocity) and the expansion in the density model. Even though both sets are power series expansions in the eccentricity, the density model does not converge as rapidly as the orbit properties. Thus for small eccentricities one may truncate at a very low order for the orbit properties, but still be required to carry out the density expansion to a higher order. In addition, it is not clear, at this time, to what order one must carry out the product of these two different expansions.

Postponing arguments on when and how to truncate, one may still list all the fourier series that are needed for a specific order m in the orbit properties expansion and n in the density expansion. They include:

$$\begin{array}{lll} c\zeta_1^i & , & cd\zeta_1^i \\ c\zeta_1^i \cos\sigma_1 & , & cd\zeta_1^i \cos\sigma_1 \\ c\zeta_1^i \sin\sigma_1 & , & cd\zeta_1^i \sin\sigma_1 \\ c\zeta_1^i\zeta_2 & , & cd\zeta_1^i\zeta_2 \end{array} \qquad (40)$$

$$c\zeta_1^i\zeta_2 \, cos \, \sigma_1 \qquad , \qquad cd\zeta_1^i\zeta_2 \, cos \, \sigma_1$$

$$c\zeta_1^i\zeta_2 \, sin \, \sigma_1 \qquad , \qquad cd\zeta_1^i\zeta_2 \, sin \, \sigma_1$$

for $i = 0$, $1 \ldots n+m$, where c is the corrective term given by equation (14) and d is the diurnal term (eq.(12)). ζ_2 is given by the relation

$$\zeta_2 = \beta \, (\rho_2 \, sin \, \sigma_1 + \sigma_2 \, cos \, \sigma_1)$$

If n and m are both set to 4, then there are a total of 108 expansions needed. This seems at first to be a rather imposing number of expansions. But drag is locally a very small force and thus the periodic effects of drag may be neglected. Therefore, only the average of these expansions needs be known. The average of a fourier expansion is simply the zeroth order term and thus only that term must be computed. One exception to this rule is the evaluation of the mixed secular forms in the time element. In this case the full expansions for $c\zeta_1^i$ and $cd\zeta_1^i$ must be evaluated. Therefore, only 18 full expansions need be determined.

If the following notations are made

$$c\zeta_1^i = \chi_0^i + \sum_{j=1}^{i+2} \left(\chi_j^i \, cos \, j\sigma_1 + \psi_j^i \, sin \, j\sigma_1 \right)$$

$$cd\zeta_1^i = \hat{\chi}_0^i + \sum_{j=1}^{i+4} \left(\hat{\chi}_j^i \, cos \, j\sigma_1 + \hat{\psi}_j^i \, sin \, j\sigma_1 \right) \tag{41}$$

and if the mean of a function $f(\sigma_1)$ with respect to σ_1 is defined by

$$\left\langle f(\sigma_1)\right\rangle_{\sigma_1} = \frac{1}{2\pi}\int_0^{2\pi} f(\sigma_1)\, d\sigma_1 \tag{42}$$

then the average values of the expansions of equation (40) are given by

$$\begin{aligned}
\left\langle c\zeta_1^i\right\rangle_{\sigma_1} &= \chi_0^i \\
\left\langle c\zeta_1^i \cos\sigma_1\right\rangle_{\sigma_1} &= \tfrac{1}{2}\chi_1^i \\
\left\langle c\zeta_1^i \sin\sigma_1\right\rangle_{\sigma_1} &= \tfrac{1}{2}\psi_1^i \\
\left\langle c\zeta_1^i\zeta_2\right\rangle_{\sigma_1} &= \frac{\beta}{2}\left(\sigma_2\psi_1^i + \rho_2\chi_1^i\right) \\
\left\langle c\zeta_1^i\zeta_2 \cos\sigma_1\right\rangle_{\sigma_1} &= \frac{\beta}{4}\left(\rho_2\psi_2^i + \sigma_2\chi_2^i + 2\sigma_2\chi_0^i\right) \\
\left\langle c\zeta_1^i\zeta_2 \sin\sigma_1\right\rangle_{\sigma_1} &= \frac{\beta}{4}\left(\sigma_2\psi_2^i - \rho_2\chi_2^i + 2\rho_2\chi_0^i\right)
\end{aligned} \tag{43}$$

The average of the expansions involving the product of c and d , can be found by replacing the uncapped ψ_j^i χ_j^i with the capped values $\hat{\psi}_j^i$, $\hat{\chi}_j^i$.

4.1 Determination of Fourier Coefficients

The coefficients of the fourier series given by equation (41) must be evaluated in some manner to complete the solution. There are several options one might take to accomplish this task. This section will be devoted to exploring these different options.

Perhaps the simplest option is to truncate the expansions on a small order of the eccentricity. This reduces the number of fourier series to be evaluated but also restricts somewhat the generality and accuracy of the solution. However, one should remember that most drag perturbed satellites do in fact have a very small eccentricity. Also a solution with a small error is better than no solution at all. If one reduces the equations by truncating the solution, then one may determine the fourier coefficients by explicit equations which are either derived by manual or computer manipulation. These explicit equations could be programmed without requiring an extremely large storage allocation.

A second option is available whereby one can evaluate all the fourier expansions without the loss of generality or accuracy. To eliminate the computer storage required of the explicit expressions, one can compute the coefficients of the fourier series in a recursive manner. The root of this procedure is an algorithm which, given the numerical value of the coefficients of two fourier series, can evaluate the coefficients for the product of the two series. The algorithm is developed from several trignometric identities and is outlined in Appendix I. With such an algorithm, all the coefficients in equation (41) can then be found in a recursive manner. For instance, the coefficients for ζ_1^2 can be found from the coefficients of ζ_1 and the coefficients for ζ_1^3 can be evaluated from the coefficients of ζ_1^2 and ζ_1, and so on. This reduces much of the instruction computer storage required by explicit expressions. Besides the advantage of being computationally simpler, this method also allows for easy updating of the drag model to include terms which effect only the *magnitude* of the perturbing force. Thus the density model can be changed easily to an expansion of arbitrary order. More importantly, if modifications of the density model, ballistic number, or coefficient of drag can be expressed as a fourier series (in σ_1), then the recursive algorithms allow for a much simpler implementation of these changes. The laborious manual derivation of these terms can be eliminated and thus a typical problem of analytical theories is partially avoided. The disadvantage to this method is the fact that no explicit equations are developed (which is ironic because this is what the method was designed to avoid). The algorithm is numerical in nature and like all numerical solutions one can find the "correct" solution but loses the insight gained from analytic, explicit solutions. In addition, the mathematical solution and the computer algorithm are so interwoven that they become inseparable. This leads us to the third option.

A recursive solution for computation of the fourier series may be possible without the loss of insight encountered with option two, above. In Mueller (reference 11) the perturbing geopotential is written in the form of a fourier series by the use of recursive relations. By a similar approach, the perturbing drag canonical forces may be developed in a recursive manner using literal expressions throughout. Thus the solution would not have the "loss of insight" typical of numerical methods and would not be tied to a computer algorithm. As an illustration, a recursive expression for the powers of ζ_1 has been developed in Appendix II. Since the powers of ζ_1 are the major components of the fourier series given by equation (40), the expressions of Appendix II more clearly define and justify the approach.

The fourth option, and the one the author feels is most viable, is an approach which is a careful blend of all the options discussed. A "careful blend" would be one that brought out the advantages of each of the options and minimizes the disadvantages.

4.2 Qualitative Aspects of Drag Perturbation

By examining the canonical PSϕ forces in the light of the new density model, one may ascertain a qualitative description of the effects of drag on the elements.

The PSϕ elements ρ_1 , ρ_4 (the energy), ρ_3 and σ_3 (related to the inclination) are perturbed secularly by the static density profile on an order of $O(\gamma)$. The static density profile refers specifically to that part of the density model which contains the a_i coefficients (eq. (11)). γ is the ratio of the magnitude of the drag force to the two-body force magnitude. The eccentricity terms, σ_2 and ρ_2 , are secularly perturbed on the order of $O(\gamma e)$ where e is eccentricity. The diurnal terms (the part containing b_i coefficients) cause additional secular perturbations of $O(\gamma e)$ in all the elements (except σ_1 which is not effected at all by the drag force[†]). Also, the static density and diurnal terms (ρ_0 in eq. (11)), give rise to quadratic and mixed secular terms of $O(\gamma)$ in the time element σ_4 . It is important to note that the neglection of the diurnal term results in errors of $O(\gamma e)$ in all the elements except σ_4 . The diurnal term

---

† In reference 1 it is shown that the motion of σ_1 (related to the true longitude) is not affected by drag perturbations.

does *not* average out in the along track position error

The correction for the static profile for the earth's oblateness and J_2 perturbations of the satellite's altitude result in secular perturbations $O(c\gamma e^2)$ where c is the magnitude of the correction $(c \leq 0.5)$. The reason for the *square* of the eccentricity is the fact that the correction is a sinusoidal function of $2\sigma_1$. But what is interesting is the coupling of the correction and the diurnal terms which results in terms of order $O(c\gamma)$. Thus the correction does not vanish for vanishing eccentricities.

The correction of the density model due to drag results in quadratic and mixed secular perturbations of order $O(c\gamma^2)$ in all the elements except σ_4 . The mixed secular terms may be neglected because of the size of the perturbation. In the time element σ_4 , the correction gives rise to cubic and mixed quadratic terms of order $O(c\gamma^3)$.

5.0 NUMERICAL STUDIES

Most, but not all, of the density model developed in section 3 has been implemented in a prototype program for the analytical drag theory. This new program is a revision of the program developed in reference 1 for the constant density model. It resides on the UNIVAC 1110 and may be executed in the interactive mode without the necessity of an overlay. The second method described in section 4.1 and outlined in Appendix I was used to generate all the necessary fourier coefficients.

Because time did not allow, the corrections in the density model due to the earth's oblateness and J_2 perturbations were not included in this program. But to test the remaining parts of the drag model, only equatorial orbits were chosen for test cases. For equatorial orbits, the neglected terms become very small and thus the errors that are observed in the tests should be realistic. As in the numerical studies of section 2, an extremely accurate numerical solution was generated which includes the J_2 oblateness and a precision drag perturbation. The density used in computing the drag force was obtained from the Jacchia model. The coefficient of drag was set to $C_d=2.2$ and the ballistic number is an average value for the shuttle $B_n = 100\ \mathrm{lb/ft^2}$ This numerical reference solution was then compared to three different analytical solutions, all of which include the short period effects of J_2 . One solution neglected drag completely, (NO DRAG) , while a second solution included drag but considered the density as a constant (CONST) The third solution was computed with the new program with the proposed density model (TOTAL) . The results are tabulated in tables III and IV. The size and shape of the different orbit test cases are given by the semi-major axis a and the eccentricity e (h_p is the perigee altitude). The position errors between the analytical and numerical solutions are displayed by the out of track error (given in meters) and the in-track error (given in kilometers). The solutions were compared about one half day or eight revolutions from the epoch of initialization.

Results of satellite orbit prediction experiments are displayed in table III. The first case is a very low, circular orbit where the drag force is extremely large and the diurnal effect is small. Therefore the major difference between the CONST and TOTAL solutions is the method in which the density model is corrected to account for the drag's lowering of the altitude. This correction does give a much better solution. The next four cases, with initial semi-major axis of 6678 km show that the TOTAL solution gives a general improvement over the NO DRAG solution of better than one digit in the out of track position and almost two digits in the in-track position. The improvement over the CONST model is substantial for the in-track position but is not so great in the out of track range. In fact, for circular orbits the CONST solution appears to be better than the TOTAL model. This inconsistency is most probably due to two interacting effects. First the constant density model results in out of track errors which are on the order of the eccentricity. This explains why the CONST and TOTAL errors are of the same order for *small* eccentricities. The long period effects of J_2 are also of the same magnitude for this relatively high satellite. These long period effects have been neglected in the analytical solutions, and thus they corrupt the estimates of the errors in the drag model. For satellites which have even higher altitudes, the out of track error is due almost entirely to the long period effects of J_2. For this reason, the test cases with a larger semi-major axis are not displayed. One can infer from these empirical results that the drag model has been refined to such an accuracy that J_2 long period effects should be included to maintain a consistent accuracy.

Another numerical test was carried out to demonstrate that the diurnal effect is indeed modeled correctly. An orbit with a semi-major axis of $a = 6878$ km and eccentricity of $e = 0.04$ is used as the test case. This represents an orbit with a perigee height of 224 km and apogee height of 775 km. The relation of the orbit with respect to the sun is a strong factor in determining how much the satellite will be perturbed. Again three analytical solutions are compared to a reference numerical solution. However, for these tests none of the solutions include the J_2 perturbation, so that the errors are purely from the drag model. The results are shown in table IV. The Jacchia model was used for the reference solution and assumes that the sun is at the vernal equinox. Two TOTAL solutions are computed; one with the sun at the vernal equinox (SPRING) and another which assumes the sun is at the first day of summer (SUMMER). As one can see the TOTAL (SPRING) solution is certainly the most accurate. A large error is incurred if the sun is assumed to be in summer when actually it is spring; as seen from the results of TOTAL (SUMMER). The numbers in parentheses are the errors when the TOTAL (SUMMER) solution is compared to a reference solution where the Jacchia also considers the sun to be in the summer.

TABLE III.- NUMERICAL SOLUTION vs ANALYTICAL SOLUTION

a (km)	e	h_p (km)	Out of track (m) / In track (km)		
			NO DRAG	CONST	TOTAL
6578	0.0	200	4891./172.8	710./12.0	15.2/0.3
6678	0.0	300	411./ 16.32	11./0.83	40.6/0.39
	0.001	293	417./ 16.48	36./1.63	40.5/0.29
	0.01	233	757./ 27.28	368./12.24	50.0/0.008
	0.02	166	3815./129.28	1664./46.08	256./2.41

TABLE IV.- DIURNAL EFFECT

Position Error	NO DRAG	CONST	TOTAL	
			SPRING	SUMMER
Out of Track (m)	3279.	169.	15.	197. (11.)
In Track (km)	59.76	25.12	2.32	13.6 (1.68)

6.0 CONCLUSIONS

In the past, the computation of the drag perturbations by an analytical method has not been feasible for two reasons. First, the various element sets chosen to base the past drag theories have never resulted in a tractable set of differential equations. This is a requirement in order to obtain concise expressions for the solution. Secondly, the analytical drag theories have failed because of their inability to model the "real world" density as a fourier series. Both of these problems are eliminated through the development of the drag differential equations in the PSϕ elements, and the subsequent development of a new density model, which closely matches a realistic density model.

The new density model has several distinct advantages. It has a rather subtle yet extremely important advantage in that the model is a power expansion in ζ_1 : i.e., the basic expansion used in Scheifele's development of the differential equations. The density model is much easier to implement in Scheifele's theory than, for instance, a model developed in power expansions of the radius†. That type of model would require additional equations in order to be placed in the basic form of the expansion in powers of ζ_1

Another advantage of the new density model is its ability to simulate *any* density model. In this report the Jacchia model was chosen for the simulations, but any other model could have been used. If more accurate density models are developed, they may also be chosen for simulation and thus the analytical drag theory can reflect the accuracy of the newly developed models.

---

† The Brouwer-Hori model is based on power series expansions in the satellite's radial distande from the center of the earth. It was found that these expansions do not converge.

Additional refinements in the drag force model should also be considered. The present theory considers the coefficient of drag and ballistic number to be constants, but they may also be allowed to vary. The frontal area of a space craft in inertial hold or in a sun pointed orientation, could be modeled as a fourier expansion in the true longitude.

Finally, it is concluded that the analytical satellite theory need not be limited by a simplified drag model. With the approaches developed in this report, it is feasible to make the accuracy of the analytical theory competitive with *precision* numerical methods, while retaining a concise formulation and quickness of execution.

REFERENCES

1. Scheifele, G., Mueller, A. and Starke, S.: "A Singularity Free Analytical Solution of Artificial Satellite Motion With Drag". ACM Technical Report TR-103, March, 1977.

2. Mueller, Alan: "The Development of the Poincaré-Similar Elements With the True Anomaly as the Independent Variable". NASA/JSC Internal Note No. 76-FM-60.

3. Scheifele, G., and Graf, O.: "Analytical Satellite Theories Based on a New Set of Canonical Elements", AIAA Paper No. 74-838, August, 1974.

4. Bond, V.R.: "An Analytical Singularity-Free Solution to the J_2 Perturbation Problem", NASA/JSC Internal Note. No. 77-FM-52, October, 1977.

5. Jacchia, L.: "New Static Models of the Thermosphere and Exosphere with Empirical Temperature Profiles", Smithsonian Astrophysical Observatory Special Report.

6. Elyasberg, P.; et al,: "Upper Atmosphere Density Determination from the Cosmos Satellite Deceleration Results", Space Research XII, p.727, Akademic-Verlag, Berlin, 1973.

7. Brouwer, D. and Hori, G.: Theoretical Evaluation of Atmospheric Drag Effects in the Motion of an Artificial Satellite, Astron, Journal, Vol. 66, No. 5, pp.193-225, 1961.

8. Mueller, A.C.: "Atmospheric Density Models", ACM Technical Report TR-106, June, 1977.

9. Santora, F.: "Drag Perturbations of Near-Circular Orbits in an Oblate Diurnal Atmosphere", AAS/AIAA Astrodynamics Conference, Paper No. AAS75-025, July, 1975.

10. Johnson, Ivan: "Matrix Inversion Computer Algorithm", JSC-MPAD Utility Program.

11. Mueller, A.C.: "Recursive Analytical Solution Describing Artificial Satellite Motion Perturbed by an Arbitrary Number of Zonal Harmonics", Paper presented at AAS/AIAA Astrodynamics Conference, September 7-9, 1977.

12. Watson, J.S., Mistretta, G.D. and Bonavito, N.L.: An Analytic Method to Account for Drag in the Vinti Satellite Theory, Celestial Mechanics, Vol. 11, No. 2, March, 1975.

APPENDIX I

If one defines the fourier series

$$A = a_0 + \sum_{i=1}^{n} (ac_i \; cos \; i\phi + as_i \; sin \; i\phi)$$

$$B = b_0 + \sum_{j=1}^{m} (bc_j \; cos \; j\phi + bs_j \; sin \; j\phi)$$

$$C = c_0 + \sum_{k=1}^{n+m} (cc_k \; cos \; k\phi + bs_k \; sin \; k\phi)$$

where

$$C = A \cdot B \quad \text{and} \quad n > m$$

then the coefficients of C are given by

$$c_0 = a_0 \cdot b_0 + \tfrac{1}{2} \sum_{i=1}^{m} (ac_i \cdot bc_i + as_i \cdot bs_i)$$

$$cc_k = a_0 \cdot bc_k + b_0 \cdot ac_k + \tfrac{1}{2} \sum_{i=1}^{n} \sum_{j=1}^{m} \left\{ \begin{bmatrix} 0 \\ ac_i \cdot bc_j - as_i \cdot bs_j \end{bmatrix} \begin{matrix} i+j \neq k \\ i+j = k \end{matrix} \right.$$

$$\left. + \begin{bmatrix} 0 \\ ac_i \cdot bc_j + as_i \cdot bs_j \end{bmatrix} \begin{matrix} |i-j| \neq k \\ |i-j| = k \end{matrix} \right\}$$

$$\dot{cs}_k = a_0 \cdot \dot{bs}_k + \dot{b}_0 \cdot cs_k + \sum_{i=1}^{n} \sum_{j=1}^{m} \left\{ \begin{bmatrix} 0 \\ ac_i \cdot bs_j + as_i \cdot bc_j \end{bmatrix} \begin{matrix} i+j \neq k \\ i+j=k \end{matrix} \right.$$

$$\left. - \begin{bmatrix} 0 \\ \frac{(j-i)}{k} (ac_i \cdot bc_j - as_i \cdot bc_j) \end{bmatrix} \begin{matrix} |i-j| \neq k \\ |i-j| = k \end{matrix} \right\}$$

Although the mathematical form of these equations appears to be quite clumsy, the algorithm can be programmed in a very concise and efficient manner. Therefore, the author has chosen also to display the FORTRAN equivalent.

FOURIER MULTIPLICATION

```
      SUBROUTINE FOURER(A,AC,AS,B,BC,BS,C,CC,CS,N,M)
      IMPLICIT REAL*8(A-H,O-Z)
      DIMENSION AC(10),AS(10),BC(10),BS(10),CC(10),CS(10)
      C=A*B
      NPM=N+M
      DO 15 I=1,NPM
      CS(I)=0.0
 15   CC(I)=0.0
      DO 20 I=1,N
      CS(I)=B*AS(I)
      CC(I)=B*AC(I)
   20 CONTINUE
      DO 30 J=1,M
      CS(J)=CS(J)+A*BS(J)
      CC(J)=CC(J)+A*BC(J)
   30 CONTINUE
       DO 10 I=1,N
       DO 10 J=1,M
       IMJ=I-J
       IPJ=I+J
       ACBC=0.5*AC(I)*BC(J)
       ASBS=0.5*AS(I)*BS(J)
       ACBS=0.5*AC(I)*BS(J)
       ASBC=0.5*AS(I)*BC(J)
       CC(IPJ)=CC(IPJ)+ACBC-ASBS
       CS(IPJ)=CS(IPJ)+ASBC+ACBS
       IF(IMJ.EQ.0) GO TO 5
       K=1
      IF(IMJ.LT.0) K=-1
       IMJ=K*IMJ
       CC(IMJ)=CC(IMJ)+ACBC+ASBS
       CS(IMJ)=CS(IMJ)+K*(ASBC-ACBS)
       GO TO 10
    5  C=C+ACBC+ASBS
   10  CONTINUE
       RETURN
       END
```

PRECEDING PAGE BLANK NOT FILMED

APPENDIX II

As defined in reference 1

$$\zeta_1 = \beta Z_1 \tag{II.1}$$

or rewriting

$$\zeta_1 = \frac{\beta}{Q} QZ_1 = \frac{\beta}{Q} e \cos \phi \tag{II.2}$$

Therefore

$$\zeta_1^n = \left(\frac{\beta}{Q}\right)^n e^n \cos^n \phi \tag{II.3}$$

The powers of a cosine can be written in a fourier series with coefficients B_k^n found by recurrence relations.

$$\cos^n \phi = \sum_{k=0}^{n} B_k^n \cos k\phi \tag{II.4}$$

or

$$e^n \cos^n \phi = \sum_{k=0}^{n} B_k^n e^{n-k} e^k \cos k\phi \tag{II.5}$$

Since ϕ is given by

$$\phi = \sigma_1 - (g+h)$$

equation (II.5) can be written as

$$e^n \cos^n \phi = \sum_{k=0}^{n} B_n^k e^{n-k} \left(\mathcal{C}_k \cos k\sigma_1 + \mathcal{S}_k \sin k\sigma_1 \right) \quad (II.6)$$

where

$$\begin{aligned} \mathcal{C}_k &= e^k \cos k(g+h) = \mathcal{C}_{k-1} \mathcal{C}_1 - \mathcal{S}_{k-1} \mathcal{S}_1 \\ \mathcal{S}_k &= e^k \sin k(g+h) = \mathcal{C}_{k-1} \mathcal{S}_1 + \mathcal{C}_1 \mathcal{S}_{k-1} \end{aligned} \quad (II.7)$$

and

$$\begin{aligned} \mathcal{C}_1 &= e \cos (g+h) = Q\rho_2 \\ \mathcal{S}_2 &= e \sin (g+h) = -Q\sigma_2 \end{aligned} \quad (II.8)$$

Therefore from equations (II.6), (II.3) and the recursive relations of (II.7) one may write a complete expression for the powers of ζ_1 in terms of a fourier expansion of the true longitude σ_1

$$\zeta_1^n = \left(\frac{\beta}{Q}\right)^n \sum_{k=0}^{n} B_n^k e^{n-k} \left(\mathcal{C}_k \cos k\sigma_1 + \mathcal{S}_k \sin k\sigma_1 \right) \quad (II.9)$$